

Original Article

Quantitative analysis of ^{18}F -NaF dynamic PET/CT cannot differentiate malignant from benign lesions in multiple myeloma

Christos Sachpekidis^{1,2}, Jens Hillengass³, Hartmut Goldschmidt^{3,4}, Hoda Anwar¹, Uwe Haberkorn^{1,5}, Antonia Dimitrakopoulou-Strauss¹

¹Clinical Cooperation Unit Nuclear Medicine, German Cancer Research Center (DKFZ), Heidelberg, Germany; ²Department of Radiology, German Cancer Research Center (DKFZ), Heidelberg, Germany; ³Department of Internal Medicine V, University Hospital Heidelberg, Heidelberg, Germany; ⁴National Center for Tumor Diseases (NCT) Heidelberg, Heidelberg, Germany; ⁵Department of Nuclear Medicine, University of Heidelberg, Heidelberg, Germany

Received May 19, 2017; Accepted July 7, 2017; Epub September 1, 2017; Published September 15, 2017

Abstract: A renewed interest has been recently developed for the highly sensitive bone-seeking radiopharmaceutical ^{18}F -NaF. Aim of the present study is to evaluate the potential utility of quantitative analysis of ^{18}F -NaF dynamic PET/CT data in differentiating malignant from benign degenerative lesions in multiple myeloma (MM). 80 MM patients underwent whole-body PET/CT and dynamic PET/CT scanning of the pelvis with ^{18}F -NaF. PET/CT data evaluation was based on visual (qualitative) assessment, semi-quantitative (SUV) calculations, and absolute quantitative estimations after application of a 2-tissue compartment model and a non-compartmental approach leading to the extraction of fractal dimension (FD). In total 263 MM lesions were demonstrated on ^{18}F -NaF PET/CT. Semi-quantitative and quantitative evaluations were performed for 25 MM lesions as well as for 25 benign, degenerative and traumatic lesions. Mean $\text{SUV}_{\text{average}}$ for MM lesions was 11.9 and mean SUV_{max} was 23.2. Respectively, $\text{SUV}_{\text{average}}$ and SUV_{max} for degenerative lesions were 13.5 and 20.2. Kinetic analysis of ^{18}F -NaF revealed the following mean values for MM lesions: $K_1 = 0.248$ (1/min), $k_3 = 0.359$ (1/min), influx (K_i) = 0.107 (1/min), FD = 1.382, while the respective values for degenerative lesions were: $K_1 = 0.169$ (1/min), $k_3 = 0.422$ (1/min), influx (K_i) = 0.095 (1/min), FD = 1.411. No statistically significant differences between MM and benign degenerative disease regarding $\text{SUV}_{\text{average}}$, SUV_{max} , K_1 , k_3 and influx (K_i) were demonstrated. FD was significantly higher in degenerative than in malignant lesions. The present findings show that quantitative analysis of ^{18}F -NaF PET data cannot differentiate malignant from benign degenerative lesions in MM patients, supporting previously published results, which reflect the limited role of ^{18}F -NaF PET/CT in the diagnostic workup of MM.

Keywords: ^{18}F -NaF, PET/CT, SUV, two-tissue compartment model, multiple myeloma, degenerative joint disease

Introduction

A renewed interest has been developed in the last years for the bone-seeking radiopharmaceutical ^{18}F -NaF, initially introduced in 1962 by Blau et al. [1]. The main reasons for this reemergence are the wide availability nowadays of PET and PET/CT scanners, the capability to quantify tracer kinetics as well as the recent worldwide shortage of $^{99}\text{Mo}/^{99\text{m}}\text{Tc}$ generators. ^{18}F -NaF is considered a highly sensitive and reliable biomarker of bone reconstruction, with potential indications in a wide range of bone diseases [2-5]. The uptake of the tracer in bone occurs by chemisorption onto hydroxyapatite, followed

by exchange with hydroxyl groups in the hydroxyapatite resulting in formation of fluoroapatite. The tracer accumulates in nearly all sites of increased new-bone formation, reflecting regional blood flow, osteoblastic activity and bone turnover [2, 6, 7].

Hawkins et al. developed a two-tissue compartment model for ^{18}F -NaF behavior, consisting of a vascular compartment, an unbound bone compartment and a bound bone mineral compartment [6]. Despite its limitations, this is considered the model that best describes the pharmacokinetics of ^{18}F -NaF in a regional level and leads to the extraction of kinetic param-

ters, which depict specific molecular processes and cannot be obtained by routine static PET studies [6, 8-11]. Nevertheless, this approach requires dynamic PET imaging for at least 60 minutes, rendering its application in everyday clinical practice difficult. The most widely used method for quantification of PET data is the calculation of standardized uptake value (SUV), a semi-quantitative parameter whose calculation requires only static imaging when the tracer has reached equilibrium. SUV represents tissue activity within a region of interest (ROI) corrected for injected activity and body weight.

The so far published data concerning the clinical utility of ^{18}F -NaF PET/CT in multiple myeloma (MM) are limited. Some studies have suggested ^{18}F -NaF PET/CT as a potential valuable tool in the diagnostics of MM [12-16]. On the other hand, our group has shown that the performance of ^{18}F -NaF PET/CT in the diagnosis as well as treatment response evaluation of MM was rather limited [17, 18]. Similarly discouraging were the results from two prospective studies from Ak et al. [19] and Bhutani et al. [20] regarding the complementary role of the modality in detecting MM lesions.

^{18}F -NaF is not tumor specific, and both malignant and non-malignant entities can exhibit increased tracer uptake [21]. In the present study we performed ^{18}F -NaF PET/CT in patients with MM. Our aim was to evaluate the potential utility of semi-quantitative and quantitative analysis of ^{18}F -NaF PET data in differentiating malignant from benign degenerative lesions in MM patients.

Materials and methods

Patients

The evaluation included 80 patients, 2 of them suffering from solitary plasmacytoma and 78 of them suffering from MM based on the criteria established by the International Myeloma Working Group (IMWG), valid at the time point of patient recruitment [22]. According to the Durie-Salmon staging system, 20 patients were suffering from stage I, 5 patients from stage II, and 53 patients from stage III MM. Sixty-seven patients had primary disease and had never received therapy for MM. Thirteen patients had recurrent disease, previously treated with chemotherapy and/or radiotherapy. Their mean

age was 59.8 years (range 38-82 years). The analysis was conducted in accordance to the declaration of Helsinki with approval of the ethical committee of the University of Heidelberg and the federal agency of radiation protection.

PET/CT data acquisition

All patients underwent ^{18}F -NaF PET/CT. For reasons of radiation protection the patients were intravenously administered with a maximum dosage of 250 MBq ^{18}F -NaF. Data acquisition consisted of two parts: the dynamic part (PET/CT studies of the lower lumbar spine and the pelvic skeleton) and the static part (whole body PET/CT). Dynamic PET/CT studies were performed for 60 minutes using a 24-frame protocol (10 frames of 30 seconds, 5 frames of 60 seconds, 5 frames of 120 seconds and 4 frames of 600 seconds). The use of lower abdomen and pelvic region for the dynamic series is justified by the fact that this anatomic area is regularly used for diagnostic bone marrow biopsies. Additional whole body static images (skull to toes) were acquired in all patients with an image duration of 2 minutes per bed position for the emission scans. A dedicated PET/CT system (Biograph mCT, 128 S, Siemens Co., Erlangen, Germany) with an axial field of view of 21.6 cm with TruePoint and TrueV, operated in a three-dimensional mode, was used for patient studies. A low-dose attenuation CT (120 kV, 30 mA) was used for the attenuation correction of the dynamic emission PET data and for image fusion. A second low-dose CT (120 kV, 30 mA) was performed after the end of the dynamic series covering the area from the skull to the toes in order to avoid patient movement after the dynamic series. The last images (55-60 minutes post-injection) were used for semi-quantitative analysis. All PET images were attenuation-corrected and an image matrix of 400×400 pixels was used for iterative image reconstruction. Iterative images reconstruction was based on the ordered subset expectation maximization algorithm (OSEM) with 6 iterations and 12 subsets.

PET/CT data analysis

Data analysis was based on: visual (qualitative) analysis, semi-quantitative evaluation based on SUV calculations, and quantitative analysis of the ^{18}F -NaF PET/CT scans. In qualitative analysis ^{18}F -NaF avid lesions were classified as

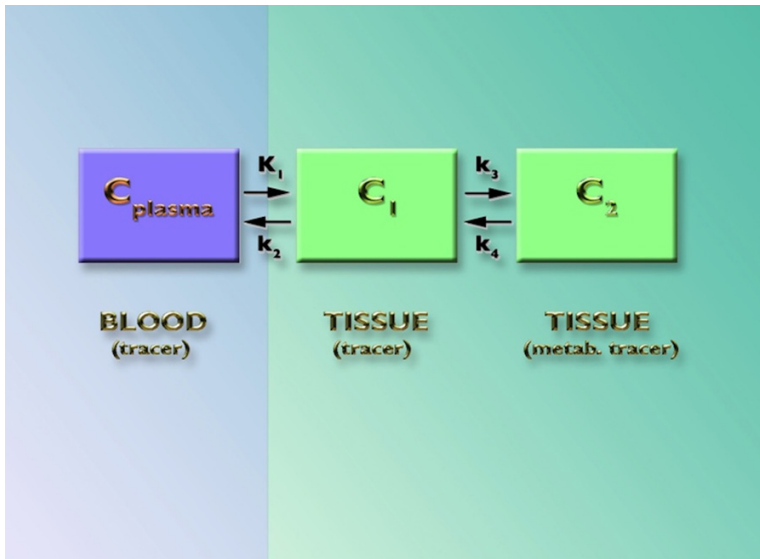


Figure 1. Schematic representation of the two-tissue compartment model for ¹⁸F-NaF. The parameters K_1 and k_2 describe the fluoride ions' clearance from plasma to the extravascular compartment, while k_3 and k_4 represent the uptake and release from the bone mineral compartment. Influx rate $K_i = K_1 \cdot k_3 \cdot (k_2 + k_3)^{-1}$ is a function of both K_1 that reflects fluoride ions' exchange with hydroxyl groups of hydroxyapatite crystal of bone, and the fraction of the tracer that undergoes specific binding to the bone mineral ($k_3 \cdot (k_2 + k_3)^{-1}$) due to the formation of fluoroapatite, and presumably represents bone remodeling rate. C_{plasma} represents the ¹⁸F-NaF concentration in plasma, C_1 represents the ¹⁸F-NaF concentration in extravascular space, and C_2 the tracer concentration in bone mineral compartment.

degenerative lesions was performed using a dedicated software and based on a two-tissue compartment model, with methods already reported in the literature and performed previously from our group [17, 18, 24-27]. The two-tissue compartment model consists of a vascular compartment, an extravascular bone compartment, and a bone mineral compartment. Two-tissue compartment modelling leads to the extraction of the kinetic parameters K_1 , k_2 , k_3 and k_4 as well as influx (K_i). The rate constants K_1 and k_2 describe the forward and reverse transport of the tracer from plasma to the extravascular component, while k_3 and k_4 represent the incorporation into and the release from the bone mineral compartment (**Figure 1**). Influx rate $K_i = K_1 \cdot k_3 \cdot (k_2 + k_3)^{-1}$ is a function of both K_1 that reflects bone blood flow,

MM and degenerative, based on the results of the underlying low-dose CT and the ¹⁸F-FDG PET/CT performed one day before, which served as reference. Briefly, only those ¹⁸F-NaF positive skeletal lesions that corresponded to lytic lesions on CT or to respective ¹⁸F-FDG positive skeletal lesions, for which another benign aetiology was excluded, were considered MM-indicative [17, 18]. Lesions were characterized as benign degenerative if the increased ¹⁸F-NaF uptake corresponded to sites adjacent to joint, osteophytes, facet joints or vertebral endplates.

and the fraction of the tracer that undergoes specific binding to the bone mineral ($k_3 \cdot (k_2 + k_3)^{-1}$). Influx rate reflects the net clearance of ¹⁸F-NaF to the bone mineral compartment and, presumably, represents bone remodelling rate [2, 9, 28].

Semi-quantitative evaluation was based on volumes of interest (VOIs) and on subsequent calculation of SUVs. VOIs were drawn with an isocontour mode (pseudo-snake) and were placed over MM lesions and benign degenerative lesions of the pelvis [23]. The SUVs 55 to 60 minutes post-injection served for the quantification of tracer data.

Besides compartment analysis, a non-compartment model was used to calculate the fractal dimension (FD). In short terms, this model measures the complexity of a dimensional structure by calculating its FD based on the box counting method. The idea is to subdivide the area into a number of square boxes and count the number of boxes containing some of the structure. FD is a parameter of heterogeneity calculated for the time activity data in each individual voxel of a VOI. Therefore, time-activity data were handled like images. The values of FD vary from 0 to 2 showing the more deterministic or chaotic distribution of the tracer activity; increased FD is indicative of a more chaotic distribution of a tracer. A subdivision of 7×7 and a maximal SUV of 20 were applied for the calculation of FD. No input function is needed for the fractal dimension model [29].

Quantitative evaluation of the dynamic ¹⁸F-NaF PET/CT data derived from MM lesions and

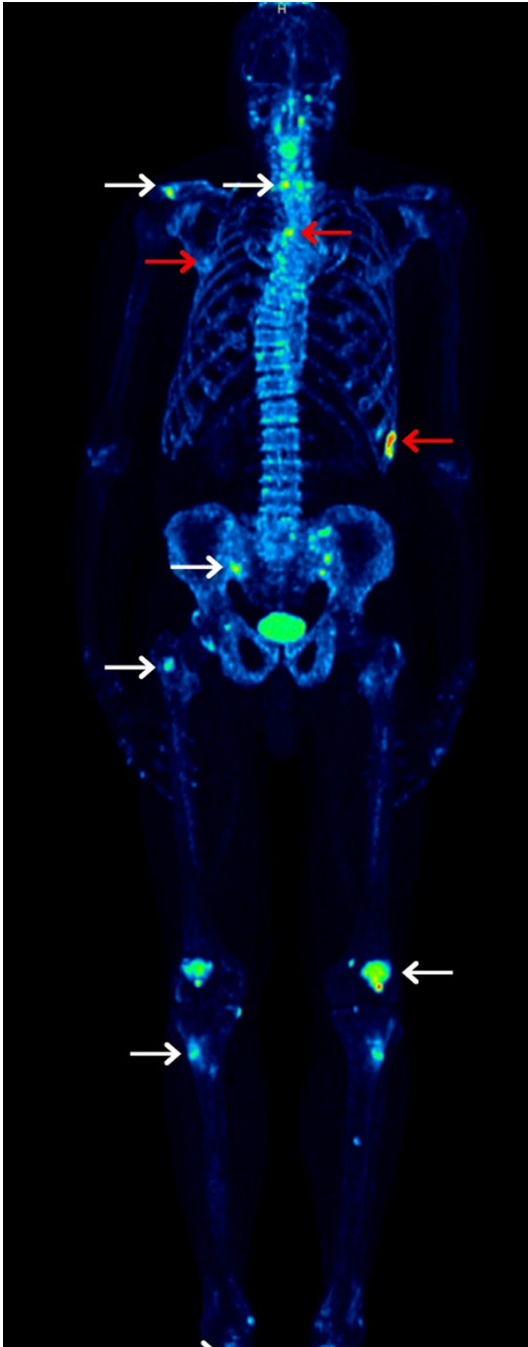


Figure 2. A 71-years old MM patient scheduled for high-dose chemotherapy and autologous stem cell transplantation. Maximum intensity projection (MIP) ¹⁸F-NaF PET/CT before therapy revealed sites of increased tracer uptake in the right scapula, the 5th thoracic vertebrae and the 8th left rib reflecting MM-indicative lesions (red arrows). Moreover, multiple sites of intense ¹⁸F-NaF uptake in the lower cervical spine, the right acromioclavicular joint, the sacroiliac joints, the right femoral neck, the knee joints and the tibial tuberosities, among others, corresponding to degenerative changes are clearly delineated (white arrows).

Table 1. Mean values of the ¹⁸F-NaF SUVs and kinetic parameters in myeloma and degenerative lesions from the pelvis, acquired with dynamic PET/CT. The units of parameters K_1 , k_2 , k_3 , k_4 and influx (K_i) are 1/min. SUVs and FD have no unit

	Myeloma lesions	Degenerative lesions
SUV _{average}	11.9	13.5
SUV _{max}	23.2	20.2
K_1	0.248	0.169
k_2^*	0.466	0.298
k_3	0.359	0.422
k_4	0.008	0.023
Influx (K_i)	0.107	0.095
FD*	1.368	1.411

*Statistically significant differences (P < 0.05).

Statistical analysis

Data were statistically evaluated using the STATA/SE 12.1 (StataCorp) software on an Intel Core (2 · 3.06 GHz, 4 GB RAM) running with Mac OS X 10.8.4 (Apple Inc., Cupertino, CA, USA). The statistical evaluation was performed using descriptive statistics, box plots, Wilcoxon rank-sum test and Spearman's rank correlation analysis. The results were considered significant for p value less than 0.05 (P < 0.05).

Results

Whole body ¹⁸F-NaF PET/CT studies

In total 263 focal MM lesions were detected with whole body ¹⁸F-NaF PET/CT. The distribution of lesions based on the Durie-Salmon classification was: one lesion in the two plasmacytoma patients, two lesions in the 20 stage I patients, ten lesions in the five stage II patients and 250 MM lesions in the 53 stage III patients. Moreover, ¹⁸F-NaF PET/CT demonstrated several degenerative changes in the patients' skeleton, which corresponded to arthritic lesions, disc osteophytes and other degenerative changes, as well as traumatic lesions (Figure 2).

Dynamic ¹⁸F-NaF PET/CT studies of the pelvis

Dynamic PET/CT revealed 25 MM indicative pelvic lesions. We performed a comparison of the SUVs and kinetic parameters between the 25 MM lesions and 25 degenerative and post-

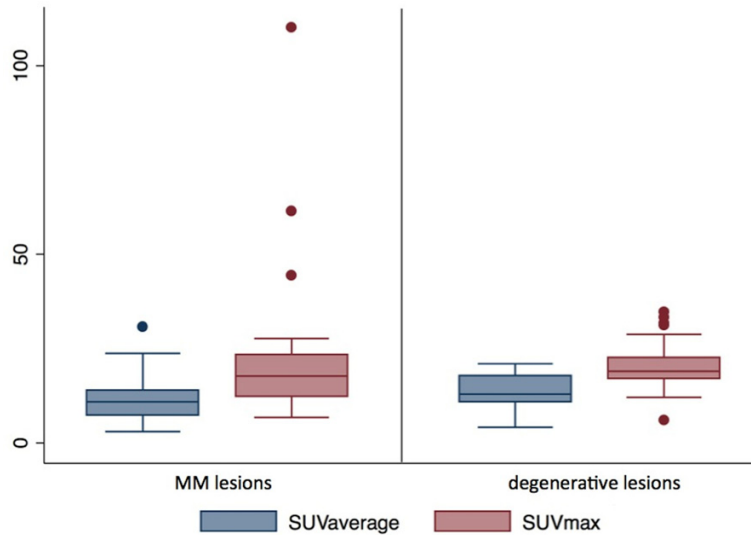


Figure 3. Box plots of ¹⁸F-NaF SUV_{average} and SUV_{max} in MM lesions and degenerative/post-traumatic lesions. No statistically significant differences between malignant and benign lesions (Wilcoxon rank-sum test, P < 0.05).

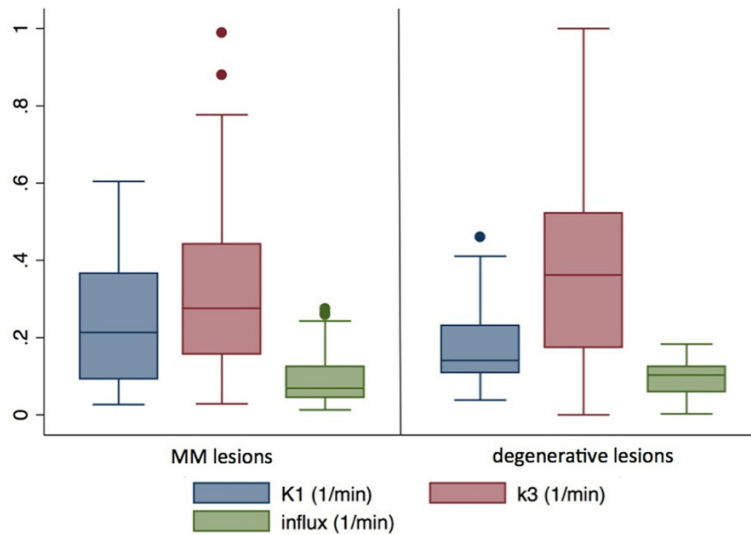


Figure 4. Box plots of ¹⁸F-NaF kinetic parameters K₁, k₃, and influx in MM lesions and degenerative/post-traumatic lesions. No statistically significant differences between malignant and benign lesions (Wilcoxon rank-sum test, P < 0.05).

traumatic lesions. Wilcoxon rank-sum analysis revealed that the parameters SUV_{average}, SUV_{max}, K₁, k₃ and influx did not show statistically significant differences between MM and degenerative lesions (Table 1; Figures 3, 4). On the other hand, FD was significantly higher for degenerative than for malignant lesions (Figure 5). Spearman's rank correlation analysis was performed between SUVs and kinetic param-

eters for the myeloma and degenerative pelvic lesions. The strongest correlations were found between FD and SUV_{average}, FD and SUV_{max}, influx and K₁, as well as between influx and SUV_{average} for the myeloma lesions (Table 2). In the case of degenerative lesions the strongest correlations were found between FD and SUV_{average}, FD and SUV_{max}, FD and influx, influx and SUV_{average} as well as between influx and K₁ (Table 3).

Discussion

An increased interest regarding the quantification of ¹⁸F-NaF PET/CT data has been documented in recent years. Several studies have analysed the distribution of ¹⁸F-NaF uptake in normal skeleton, degenerative changes and malignant lesions, using semi-quantitative SUV measurements. Sabbah et al. created an atlas of ¹⁸F-NaF SUVs for normal bone, degenerative benign lesions and metastatic lesions based on a cohort of 129 oncological patients, most of which suffered from prostate cancer and only 2 of them from MM. The authors found that osseous metastases demonstrated statistically significant higher SUV_{max} than degenerative lesions [30]. Win et al. showed in a group of 11 patients without bone disease that various skeletal sites have different normal SUV_{max}, with vertebral bodies tending to show the highest values [31]. In a study involving 17 castrate resistant prostate cancer patients, Muzahir et al. measured SUV_{max} in 65 metastatic and 56 degenerative joint disease sites. Despite some overlap of SUV_{max} range between benign and metastatic sites, the authors found that a SUV_{max} over 50 always re-

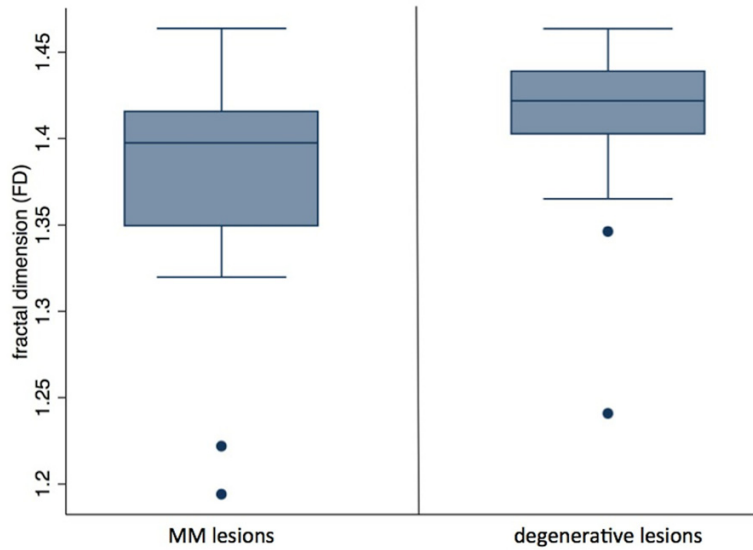


Figure 5. Box plots of ¹⁸F-NaF fractal dimension (FD) in MM lesions and degenerative/post-traumatic lesions. FD in benign skeletal lesions was significantly higher than in malignant lesions (Wilcoxon rank-sum test, P < 0.05).

Table 2. Results of the correlation analysis between ¹⁸F-NaF quantitative and semi-quantitative (SUVs) parameters regarding MM lesions. The units of parameters K₁, k₂, k₃, k₄ and influx (K_i) are 1/min. SUVs and FD have no unit

	SUV _{average}	SUV _{max}	K ₁	k ₃	Influx (K _i)
SUV _{max}	0.9115*				
K ₁	0.5131*	0.4254*			
k ₃	0.5723*	0.4169*	0.3531		
Influx (K _i)	0.6631*	0.5931*	0.9108*	0.4846*	
FD	0.9700*	0.8946*	0.5346*	0.5038*	0.6354*

*Statistically significant correlations (P < 0.05).

Table 3. Results of the correlation analysis between ¹⁸F-NaF quantitative and semi-quantitative (SUVs) parameters regarding degenerative lesions. The units of parameters K₁, k₂, k₃, k₄ and influx (K_i) are 1/min. SUVs and FD have no unit

	SUV _{average}	SUV _{max}	K ₁	k ₃	Influx (K _i)
SUV _{max}	0.8562*				
K ₁	0.5015*	0.5577*			
k ₃	0.3762	0.3323	0.2285		
Influx (K _i)	0.7846*	0.6338*	0.7846*	0.4208	
FD	0.9369*	0.7877*	0.4769*	0.4423	0.7908*

*Statistically significant correlations (P < 0.05).

presented a bone metastasis and that a SUV_{max} below 11 always represented a site of degenerative joint disease [32]. Oldan et al. showed in a group of 47 prostate cancer patients that

SUV_{average} in metastatic lesions is higher than in degenerative lesions, but there was significant SUV_{average} overlap between the two lesion groups and the difference was not statistically significant [33].

A method for evaluating the kinetics of ¹⁸F-NaF was developed by Hawkins et al. based on a two-tissue compartment model consisting of the plasma space, an unbound bone compartment and a bound bone compartment [6]. This is the first study using a combination of semi-quantitative and quantitative analysis for differentiation of malignant from benign lesions in MM by means of dynamic ¹⁸F-NaF PET/CT. We have shown that there are no statistically significant differences between MM and benign degenerative/traumatic skeletal disease regarding both SUVs and absolute kinetic parameters, derived after application of two-tissue compartment modelling. In a molecular level, these findings reflect that the level of ¹⁸F-NaF uptake and thus, the underlying osteoblastic activity (SUV_{average}, SUV_{max}), the tracer transport rate from plasma to the extravascular component (K₁), its incorporation into the bone mineral compartment (k₃), as well as the Ca²⁺ influx, bone apposition rate and, presumably, bone remodelling rate (influx-K_i) do not show significant differences between malignant myeloma and benign degenerative/traumatic lesions. Interestingly,

the application of a non-compartmental approach based on chaos theory for the analysis of dynamic PET data, led to the conclusion that the degree of tissue heteroge-

neity, reflected by fractal dimension (FD), is significantly higher in degenerative changes than in MM lesions.

Our results are not in accordance with those of the previously reported studies, comparing metastatic and benign bone lesions. Since the uptake of ^{18}F -NaF indicates osteoblastic activity, this discordance could be attributed to the nature of the osseous, malignant lesions studied. The majority of the patients in the reported studies were suffering from prostate cancer, which induces, most frequently, pure osteoblastic metastases. In contrary, the hallmark of MM is the osteolytic lesion [34], with the accumulation of ^{18}F -NaF taking place in the accompanying, sometimes minimal, reactive osteoblastic changes [35].

Nevertheless, the here presented data are complementary and in line with previous results published from our group, concerning the role of ^{18}F -NaF PET/CT in MM diagnostics. In a study involving 60 MM patients we have shown that ^{18}F -NaF PET/CT detected less focal MM lesions than ^{18}F -FDG PET/CT, its specificity was low and it could not depict diffuse bone marrow involvement, thus, it could not provide significant information to the diagnostic approach of MM patients, who had already gone through ^{18}F -FDG PET/CT [17]. Further, ^{18}F -NaF PET/CT did not add significantly to ^{18}F -FDG PET/CT in treatment response evaluation of a group of 34 primary MM patients undergoing high-dose chemotherapy followed by autologous stem cell transplantation [18]. Those results, as well as two recently published results from other groups regarding the performance of ^{18}F -NaF PET/CT in MM [19, 20], indicate that the contribution of ^{18}F -NaF PET/CT in this neoplastic plasma cell disorder is rather limited, provided that ^{18}F -FDG PET/CT is involved in the MM diagnostic workup. However, ^{18}F -NaF provides general information regarding bone remodelling and the patient's skeletal history.

Correlation analysis revealed significant, positive correlations between the degree of ^{18}F -NaF uptake ($\text{SUV}_{\text{average}}$, SUV_{max}) and fluoride bone influx rate for both MM and degenerative lesions. This finding is in agreement with the results of Brenner et al., who found very strong positive linear correlation between ^{18}F -NaF SUV and influx rate obtained by both Patlak analysis and nonlinear regression in patients with

bone tumors after tumor resection and bone graft surgery [8]. Interestingly, the strongest correlations were observed between $\text{SUV}_{\text{average}}$ and SUV_{max} and FD, implying that the degree of ^{18}F -NaF uptake increases with the degree of tissue heterogeneity both in malignant and degenerative lesions.

Our study carries some limitations. Firstly, the vast majority of the PET/CT positive MM-indicative findings were not histopathologically confirmed, which is, however, usually not possible in the clinical setting. Nonetheless, all lesions were correlated with respective findings on underlying CT, a standard technique in MM diagnostics, as well as on ^{18}F -FDG PET/CT, whose role is increasingly recognised in the diagnosis and treatment response evaluation of MM [36, 37]. Secondly, the studied population was not homogeneous, since it involved a combination of treated and non-treated MM patients. Nevertheless, the use of the ^{18}F -FDG PET/CT as well as of the underlying CT information helped us correctly identify and exclude from characterisation as MM-indicative those ^{18}F -NaF avid lesions that represented treatment-related changes. Finally, despite the fact that a two-bed position protocol, which allows the study of a relatively large field of view of 44 cm, was used, the dynamic PET/CT acquisition was confined only in the anatomic area of the pelvis [38]. However, whole-body dynamic studies cannot be performed. The expected advent of new PET/CT scanners, which will allow dynamic studies over several bed positions by using a continuous bed movement, will facilitate the use of dynamic PET protocols and reduce the whole acquisition time.

Conclusion

This single-center study has shown that semi-quantitative and quantitative analysis of ^{18}F -NaF dynamic PET/CT data cannot differentiate malignant from benign degenerative and traumatic lesions in MM patients. These findings support previously published results, concerning the application of ^{18}F -NaF PET/CT in MM, and indicate that the role of ^{18}F -NaF PET/CT in the diagnostic workup of MM patients is rather limited.

Acknowledgements

The study was part of a special research area project (SFB TRR 79) funded by the German Research Foundation.

Disclosure of conflict of interest

None.

Address correspondence to: Dr. Christos Sachpekidis, Clinical Cooperation Unit Nuclear Medicine, German Cancer Research Center, Im Neuenheimer Feld 280, D-69210, Heidelberg, Germany. E-mail: christos_saxpe@yahoo.gr; c.sachpekidis@dkfz-heidelberg.de

References

[1] Blau M, Nagler W, Bender MA. Fluorine-18: a new isotope for bone scanning. *J Nucl Med* 1962; 3: 332-334.

[2] Czernin J, Satyamurthy N, Schiepers C. Molecular mechanisms of bone ¹⁸F-NaF deposition. *J Nucl Med* 2010; 51: 1826-1829.

[3] Segall G, Delbeke D, Stabin MG, Even-Sapir E, Fair J, Sajdak R, Smith GT; SNM. SNM practice guideline for sodium ¹⁸F-fluoride PET/CT bone scans 1.0. *J Nucl Med* 2010; 51: 1813-1820.

[4] Beheshti M, Mottaghy FM, Payche F, Behrendt FF, Van den Wyngaert T, Fogelman I, Strobel K, Celli M, Fanti S, Giammarile F, Krause B, Langsteger W. (18)F-NaF PET/CT: EANM procedure guidelines for bone imaging. *Eur J Nucl Med Mol Imaging* 2015; 42: 1767-1777.

[5] Hillner BE, Siegel BA, Hanna L, Duan F, Quinn B, Shields AF. ¹⁸F-fluoride PET used for treatment monitoring of systemic cancer therapy: results from the national oncologic PET registry. *J Nucl Med* 2015; 56: 222-228.

[6] Hawkins RA, Choi Y, Huang SC, Hoh CK, Dahlbom M, Schiepers C, Satyamurthy N, Barrio JR, Phelps ME. Evaluation of the skeletal kinetics of fluorine-18-fluoride ion with PET. *J Nucl Med* 1992; 33: 633-642.

[7] Grant FD, Fahey FH, Packard AB, Davis RT, Alavi A, Treves ST. Skeletal PET with ¹⁸F-fluoride: applying new technology to an old tracer. *J Nucl Med* 2008; 49: 68-78.

[8] Brenner W, Vernon C, Muzi M, Mankoff DA, Link JM, Conrad EU, Eary JF. Comparison of different quantitative approaches to ¹⁸F-fluoride PET scans. *J Nucl Med* 2004; 45: 1493-1500.

[9] Schiepers C, Nuyts J, Bormans G, Dequeker J, Bouillon R, Mortelmans L, Verbruggen A, De Roo M. Fluoride kinetics of the axial skeleton measured in vivo with fluorine-18-fluoride PET. *J Nucl Med* 1997; 38: 1970-1976.

[10] Blake GM, Park-Holohan SJ, Cook GJ, Fogelman I. Quantitative studies of bone with the use of ¹⁸F-fluoride and ^{99m}Tc-methylene diphosphonate. *Semin Nucl Med* 2001; 31: 28-49.

[11] Wong KK, Piert M. Dynamic bone imaging with ^{99m}Tc-labeled diphosphonates and ¹⁸F-NaF: mechanisms and applications. *J Nucl Med* 2013; 54: 590-599.

[12] Tan E, Weiss BM, Mena E, Korde N, Choyke PL, Landgren O. Current and future imaging modalities for multiple myeloma and its precursor states. *Leuk Lymphoma* 2011; 52: 1630-1640.

[13] Kurdziel KA, Shih JH, Apolo AB, Lindenberg L, Mena E, McKinney YY, Adler SS, Turkbey B, Dahut W, Gulley JL, Madan RA, Landgren O, Choyke PL. The kinetics and reproducibility of ¹⁸F-sodium fluoride for oncology using current PET camera technology. *J Nucl Med* 2012; 53: 1175-1184.

[14] Nishiyama Y, Tateishi U, Shizukuishi K, Shishikura A, Yamazaki E, Shibata H, Yoneyama T, Ishigatsubo Y, Inoue T. Role of ¹⁸F-fluoride PET/CT in the assessment of multiple myeloma: initial experience. *Ann Nucl Med* 2013; 27: 78-83.

[15] Xu F, Liu F, Pastakia B. Different lesions revealed by ¹⁸F-FDG PET/CT and ¹⁸F-NaF PET/CT in patients with multiple myeloma. *Clin Nucl Med* 2014; 39: e407-409.

[16] Oral A, Yazici B, Ömür Ö, Comert M, Saydam G. ¹⁸F-FDG and ¹⁸F-NaF PET/CT findings of a multiple myeloma patient with thyroid cartilage involvement. *Clin Nucl Med* 2015; 40: 873-876.

[17] Sachpekidis C, Goldschmidt H, Hose D, Pan L, Cheng C, Kopka K, Haberkorn U, Dimitrakopoulou-Strauss A. PET/CT studies of multiple myeloma using (18)F-FDG and (18)F-NaF: comparison of distribution patterns and tracers' pharmacokinetics. *Eur J Nucl Med Mol Imaging* 2014; 41: 1343-1353.

[18] Sachpekidis C, Hillengass J, Goldschmidt H, Wagner B, Haberkorn U, Kopka K, Dimitrakopoulou-Strauss A. Treatment response evaluation with ¹⁸F-FDG PET/CT and ¹⁸F-NaF PET/CT in multiple myeloma patients undergoing high-dose chemotherapy and autologous stem cell transplantation. *Eur J Nucl Med Mol Imaging* 2017; 44: 50-62.

[19] Ak I, Onner H, Akay OM. Is there any complementary role of F-18 NaF PET/CT in detecting of osseous involvement of multiple myeloma? A comparative study of F-18 FDG PET/CT and F-18 FDG NaF PET/CT. *Ann Hematol* 2015; 94: 1567-1575.

[20] Bhutani M, Turkbey B, Tan E, Korde N, Kwok M, Manasanch EE, Tajeja N, Mailankody S, Roschewski M, Mulquin M, Carpenter A, Lamping E, Minter AR, Weiss BM, Mena E, Lindenberg L, Calvo KR, Maric I, Usmani SZ, Choyke PL, Kurdziel K, Landgren O. Bone marrow abnormalities and early bone lesions in multiple myeloma and its precursor disease: a prospective study using functional and morphologic imaging. *Leuk Lymphoma* 2016; 57: 1114-1121.

[21] Bastawrous S, Bhargava P, Behnia F, Djang DS, Haseley DR. Newer PET application with an

- old tracer: role of ¹⁸F-NaF skeletal PET/CT in oncologic practice. *Radiographics* 2014; 34: 1295-1316.
- [22] International Myeloma Working Group. Criteria for the classification of monoclonal gammopathies, multiple myeloma and related disorders: a report of the International Myeloma Working Group. *Br J Haematol* 2003; 121: 749-757.
- [23] <http://www.pmod.com/files/download/v31/doc/pbas/4729.htm>.
- [24] Ohtake T, Kosaka N, Watanabe T, Yokoyama I, Moritan T, Masuo M, Iizuka M, Kozeni K, Momose T, Oku S. Noninvasive method to obtain input function for measuring tissue glucose utilization of thoracic and abdominal organs. *J Nucl Med* 1991; 32: 1432-1438.
- [25] Burger C, Buck A. Requirements and implementations of a flexible kinetic modeling tool. *J Nucl Med* 1997; 38: 1818-1823.
- [26] Mikolajczyk K, Szabatin M, Rudnicki P, Grodzki M, Burger C. A Java environment for medical image data analysis: initial application for brain PET quantitation. *Med Inform* 1998; 23: 207-214.
- [27] Cheng C, Alt V, Dimitrakopoulou-Strauss A, Pan L, Thormann U, Schnettler R, Weber K, Strauss LG. Evaluation of new bone formation in normal and osteoporotic rats with a 3-mm femur defect: functional assessment with dynamic PET-CT (dPET-CT) using a 2-deoxy-2 [(18)F] fluoro-D-glucose (18F-FDG) and 18F-fluoride. *Mol Imaging Biol* 2013; 15: 336-344.
- [28] Frost ML, Fogelman I, Blake GM, Marsden PK, Cook G Jr. Dissociation between global markers of bone formation and direct measurement of spinal bone formation in osteoporosis. *J Bone Miner Res* 2004; 19: 1797-1804.
- [29] Dimitrakopoulou-Strauss A, Strauss LG, Mikolajczyk K, Burger C, Lehnert T, Bernd L, Ewerbeck V, et al. On the fractal nature of positron emission tomography (PET) studies. *World J Nucl Med* 2003; 4: 306-313.
- [30] Sabbah N, Jackson T, Mosci C, Jamali M, Minamoto R, Quon A, Mittra ES, Iagaru A. 18F-sodium fluoride PET/CT in oncology: an atlas of SUVs. *Clin Nucl Med* 2015; 40: e228-231.
- [31] Win AZ, Aparici CM. Normal SUV values measured from NaF18-PET/CT bone scan studies. *PLoS One* 2014; 9: e108429.
- [32] Muzahir S, Jeraj R, Liu G, Hall LT, Rio AM, Perk T, Jaskowiak C, Perlman SB. Differentiation of metastatic vs degenerative joint disease using semi-quantitative analysis with (18)F-NaF PET/CT in castrate resistant prostate cancer patients. *Am J Nucl Med Mol Imaging* 2015; 5: 162-168.
- [33] Oldan JD, Hawkins AS, Chin BB. (18)F sodium fluoride PET/CT in patients with prostate cancer: quantification of normal tissues, benign degenerative lesions, and malignant lesions. *World J Nucl Med* 2016; 15: 102-108.
- [34] Walker RC, Brown TL, Jones-Jackson LB, De Blanche L, Bartel T. Imaging of multiple myeloma and related plasma cell dyscrasias. *J Nucl Med* 2012; 53: 1091-1101.
- [35] Even-Sapir E, Mishani E, Flusser G, Metser U. 18F-Fluoride positron emission tomography and positron emission tomography/computed tomography. *Semin Nucl Med* 2007; 37: 462-469.
- [36] Rajkumar SV, Dimopoulos MA, Palumbo A, Blade J, Merlini G, Mateos MV, Kumar S, Hillengass J, Kastritis E, Richardson P, Landgren O, Paiva B, Dispenzieri A, Weiss B, LeLeu X, Zweegman S, Lonial S, Rosinol L, Zamagni E, Jagannath S, Sezer O, Kristinsson SY, Caers J, Usmani SZ, Lahuerta JJ, Johnsen HE, Beksac M, Cavo M, Goldschmidt H, Terpos E, Kyle RA, Anderson KC, Durie BG, Miguel JF. International Myeloma Working Group updated criteria for the diagnosis of multiple myeloma. *Lancet Oncol* 2014; 15: e538-e548.
- [37] Kumar S, Anderson KC, Durie B, Landgren O, Moreau P, Munshi N, Lonial S, Bladé J, Mateos MV, Dimopoulos M, Kastritis E, Boccadoro M, Orłowski R, Goldschmidt H, Spencer A, Hou J, Chng WJ, Usmani SZ, Zamagni E, Shimizu K, Jagannath S, Johnsen HE, Terpos E, Reiman A, Kyle RA, Sonneveld P, Richardson PG, McCarthy P, Ludwig H, Chen W, Cavo M, Harousseau JL, Lentzsch S, Hillengass J, Palumbo A, Orfao A, Rajkumar SV, San Miguel J, Avet-Loiseau H. International Myeloma Working Group consensus criteria for response and minimal residual disease assessment in multiple myeloma. *Lancet Oncol* 2016; 17: e328-e346.
- [38] Dimitrakopoulou-Strauss A, Pan L, Strauss LG. Quantitative approaches of dynamic FDG-PET and PET/CT studies (dPET/CT) for the evaluation of oncological patients. *Cancer Imaging* 2012; 12: 283-289.